Food Science of Animal Products

Research Article

Preparation and characterization of Pacific salmon protein antifreeze emulsion

Zhe Xu[1,2], Yikun Xu[2], Xuguang Mo[2], Ziyu Zhang[2], Haoran Wu[2], Yidi Luo[2], Tingting Li[1,2] ✉

[1] *Dalian Xinghai Bay Laboratory, Dalian 116034, China*
[2] *Key Laboratory of Biotechnology and Bioresources Utilization, Ministry of Education, College of Life Sciences, Dalian Minzu University, Dalian 116600, China*

✉Address correspondence to Tingting Li, jwltt@dlnu.edu.cn

Received: March 6, 2026; Revised: March 23, 2026; Accepted: April 29, 2026

Abstract: Temperature fluctuations during storage and transportation can compromise the quality of aquatic products. In this study, Pacific salmon bone collagen (SBC) was extracted from Pacific salmon bones and used to prepare a salmon bone collagen emulsion (SBCE). Pacific salmon fillets were treated with SBC, and their antifreeze activity was measured in terms of texture characteristics, moisture retention, color difference changes, and flavor stability during multiple freeze-thaw cycles. Subsequently, the physicochemical stability of emulsions with different oil contents was evaluated under ambient storage, centrifugation, and freeze-thaw challenging. Antifreeze efficacy was evaluated by subjecting the Pacific salmon fillets with SBCEs during freeze-thaw cycles. Studied the potential of SBCE freezing and thawing to maintain the quality of Pacific salmon. The results showed that emulsions containing 60%–70% oil phase exhibited the highest stability. Among formulations, SBCE2.0 most effectively preserved texture, reduced moisture loss, and limited denaturation and aggregation of myofibrillar proteins. Overall, SBCE significantly alleviated ice-induced quality loss in fish product and shows promise as a natural antifreeze agent for aquatic products.

Keywords: Pacific salmon bone collagen; myofibrillar protein oxidation; freeze-thaw stability; antifreeze emulsion

Citation: Z. Xu, Y. K. Xu, X. G. Mo, et al., Preparation and characterization of Pacific salmon protein antifreeze emulsion, Food Sci. Anim. Prod. 4 (2026) 9240168. https://doi.org/10.26599/FSAP.2026.9240168.

1 Introduction

Fish is valued for its delicate texture and nutritional quality but is highly susceptible to deterioration during postharvest handling and storage. Although freezing is widely used for preservation, temperature fluctuations during storage and transportation can promote ice crystallization, which may induce protein degradation[1]. To minimize freeze induced damage, cryoprotectants such as sucrose and sorbitol are widely used in commercial frozen seafood[2–3]. However, these additives introduce undesirable attributes, including excessive sweetness, high caloric value, and potential off-flavors, which limit consumer acceptance and further application[3–4]. Consequently, there is a need for alternative cryoprotectants that are natural, safe, and capable of maintaining food quality without compromising nutritional and sensory properties.

Edible coatings prepared from natural polymers are promising alternatives for extending the shelf life of perishable foods without compromising nutritional value[5]. Antifreeze proteins (AFPs), first identified South Sea fish, are a class of proteins capable of binding to ice crystal surfaces, inhibiting recrystallization, and protecting cellular structures during freezing[6]. These properties reduce ice induced damage and help maintain the quality of frozen foods. However, their industrial application remains limited due to high cost, instability, and challenges in large-scale production. Unlike single component edible coatings or AFPs, antifreeze emulsions integrate the advantages of colloidal dispersion systems and bioactive components, their oil-water interface structure can physically isolate fish muscle tissue from external ice crystal invasion, while the bioactive ingredients in the system exert targeted antifreeze effects. Such emulsions are typically composed of proteins, oils, water, and antioxidants, providing excellent freeze-thaw stability under low temperature conditions. In contrast, emulsion-based systems have improved stability and enhanced compatibility with food matrices, facilitating the preservation of the original flavor and texture of frozen products. These characteristics make antifreeze emulsions promising cryoprotectants for frozen food preservation.

Collagen in the emulsion system can stabilize the oil-water interface through electrostatic adsorption and steric hindrance, forming a compact interface facial film that prevents droplet coalescence[7]. In addition, collagen itself exhibits antifreeze capacity. Previous study has reported that specific peptide segments in collagen can bind to the surface of ice crystals through hydrogen bonding, inhibiting ice crystal growth and recrystallization[8]. This dual-functional property of being both an emulsion stabilizer and an active antifreeze ingredient makes collagen an ideal core material for preparing antifreeze emulsions, as it does not require additional antifreeze additives, simplifying emulsion formulations while enhancing the overall antifreeze effect. The fish bones generated during Pacific salmon processing are usually discarded or used as animal feed, resulting in resource waste and environmental pollution. Extracting collagen from Pacific salmon bones can not only achieve high value utilization of fishery by-products, but also reduce production costs. In addition, as a fish derived collagen, Pacific salmon bone collagen (SBC) has similar amino acid composition and structural compatibility with its muscle tissue, it

can improve the adhesion and bioavailability of the emulsion on the fish fillet surface, a key differentiating advantage compared with terrestrial animal-derived collagen or plant proteins, these materials are commonly used in existing antifreeze emulsions but have poor compatibility with aquatic food matrices.

Therefore, this study aimed to develop a Pacific SBC-based antifreeze emulsion (SBCE) and assess its effects on the physicochemical quality of Pacific salmon fillets during consecutive freeze-thaw cycles. The stability of SBCEs with different water-to-oil (W/O) ratios was evaluated, and their ability to preserve texture, mitigate protein oxidation, and maintain structural integrity was assessed. The result from this study provides a feasible cryoprotective strategy while enabling value-added utilization of aquatic by-products.

2 Materials and methods

2.1 Materials

Pacific salmon was purchased from Dalian Rich Foods Co., Ltd. (Dalian, China). Bovine serum albumin (BSA), pepsin was purchased from Shanghai McLean Biochemical Technology Co., Ltd. (Shanghai, China). Algae oil was purchased from Jiangsu Yuanda Xianle Pharmaceutical Co., Ltd. (Yancheng, China). All of the chemicals and reagents used were of analytical grade.

2.2 Preparation of Pacific SBC and sodium dodecyl sulfate-polyacrylamide gel electrophoresis (SDS-PAGE)

Pacific SBC was isolated and obtained with reference to a previously reported method, with minor modifications made during the extraction process[9]. The bones were carefully removed from Pacific salmon and dried. Add 0.1 mol/L NaOH into the bone sample at ratio of 5:1 (*m*/*m*), and the mixture was stirred at 4 °C for 8 h, followed by washing and thermal drying. Five volumes of 0.25 mol/L ethylenediaminetetraacetic acid-2Na were added to the sample, and the mixture was stirred at 4 °C for 12 h, then washed with distilled water to neutral and drained. Then, 0.5 mol/L acetic acid solution were added to the bone sample at ratio of 5:1 (*m*/*m*), and gastric protease (10 000 U/g) was added at 1.6% (*m*/*m*, based on bone mass). The mixture was stirred at 4 °C for 24 h and then filtered. The residue was extracted twice more using fresh 0.5 mol/L acetic acid solution under the same conditions, the three extractions were collected and combined, then suspended into the normal saline and stirred continuously to allow the precipitation. The precipitate was then dissolved in a 0.5 mol/L acetic acid solution and centrifuged at 9 000 × *g* for 20 min to collect the precipitate. Dialysis was performed against 0.1 mol/L acetic acid solution and ultrapure water for 24 h, with water change every 8 h. SBC was collected by freeze-drying at the end of experiment.

SDS-PAGE was performed according to the protocol described in the literature with slight modifications[10]. A polyacrylamide gel composed of 8% separating gel and 4% stacking gel was used for measurement. The collagen solution (2 mg/mL) and loading buffer were mixed at a ratio of 4:1 (*V*/*V*) and boiled for 10 min. Then, 10 μL of collagen mixed solution was loaded into the sample well for electrophoresis. After electrophoresis, the gel was stained with Coomassie Brilliant Blue R-250 and subsequently destained using a solution containing 5% (*V*/*V*) ethanol and 10% (*V*/*V*) acetic acid until the bands became clear. The resulting images were obtained using a luminescence imaging system (Tanon-5200, Shanghai Tianneng Bioengineering Technology Co., Ltd., Shanghai, China).

2.3 Sample pre-treatment

Fresh Pacific salmon was transported to the laboratory on ice within after slaughter. The fillets were assigned to the following treatments: Con (fresh fish as control), NCon (fish stored in aqueous solution without additives), SBC0.5 (immersed in 0.5 mg/mL Pacific SBC), SBC1.0 (1 mg/mL), SBC2.0 (2 mg/mL), SBC3.0 (3 mg/mL), and PCon (4% sucrose + 4% sorbitol, *m*/*m*, as positive control). All samples were frozen at –20 °C for 24 h and then thawed at 4 °C for 12 h until the core temperature reached 0–4 °C. Each group underwent five freeze-thaw cycles.

2.4 Determination of physical properties

2.4.1 Texture properties

Texture analysis was performed using a texture analyzer (TA.XT Plus, Stable Micro Systems, Godalming, UK). Fish fillet samples were cut into cubes (1 cm^3), and ten replicates were measured for each treatment. A P/50 cylindrical probe was utilized for the texture measurement, with the compression strain fixed at 30% and the test speed adjusted to 1.0 mm/s; relevant texture parameters (hardness, springiness, cohesiveness, and adhesiveness) were subsequently documented. This method can be applied to SBC and SBCE.

2.4.2 Scanning electron microscopy (SEM) observation

For the treated fillets, SEM characterization was performed in accordance with existing literature, with minor procedural modifications adopted during the test[11]. Thawed fillets were cut into 3 mm × 3 mm × 3 mm cubes and dehydrated in graded ethanol. Samples were fixed in 2.5% glutaraldehyde, gold-coated, and imaged using a scanning electron microscope (S-4800, Hitachi Ltd., Japan) at 400× magnification and 5 kV. This method can be applied to SBC and SBCE.

2.4.3 Moisture loss

Fish fillets were thawed at 4 °C until the core temperature reached 4 °C, and surface moisture was gently removed using Kimwipes. Samples were weighed prior to and following thawing, with these weights reported as m_0 (g, pre-thaw) and m_1 (g, post-thaw), respectively[12]. Thawing loss rate was computed via equation (1):

$$\text{Thawing loss rate}\ (\%) = \frac{m_0 - m_1}{m_0} \times 100 \quad (1)$$

Moisture loss associated with the centrifugation process was assessed by adapting established literature methods[13]. Fish fillet weights were measured before (m_2, g) and after (m_3, g) centrifugation, and centrifugal moisture loss rate was determined using equation (2):

$$\text{Centrifugal loss rate}\ (\%) = \frac{m_2 - m_3}{m_2} \times 100 \quad (2)$$

Cooking moisture loss rate was evaluated with minor modifications to published protocols[13]. Thawed fillets were enclosed in polyethylene bags, steamed at 80 °C for a 15 min duration. Samples were cooled to 25 °C by removing surface moisture. Each sample's weight was reported both before (m_4, g) and after (m_5, g) the cooking process, and cooking loss was computed using equation (3):

$$\text{Cooking loss rate}\ (\%) = \frac{m_4 - m_5}{m_4} \times 100 \quad (3)$$

2.4.4 Color

The processed Pacific salmon was cut into pieces measuring 20 mm × 20 mm × 15 mm, and the color parameters (the brightness (L^*), redness (a^*), and yellowness values (b^*)) of the fish pieces were measured using a CR-400 colorimeter (Konica Minolta, Japan). Six parallel measurements were repeated for each sample[14]. This method can be applied to SBC and SBCE.

2.4.5 Electronic nose (E-nose)

An E-nose (PEN3, Insent, Atsugi, Japan) was used to evaluate volatile profiles of fish fillets. Homogenized samples were sealed in headspace vials, and the sampling needle was inserted through the vial septum. Each measurement consisted of a 60 s acquisition period following a 60 s purge phase, with the carrier gas flow rate set at 200 mL/min. This method can be applied to SBC and SBCE.

2.5 Preparation of SBCE

The antifreeze emulsion was prepared according to a previously reported method with minor modifications[15]. Freeze dried Pacific SBC was dissolved in water to formulate solutions with concentrations ranging from 0.5 to 3.0 mg/mL. Algal oil was incorporated at oil phase volume fractions (φ) between 0.1 and 0.7, and the mixtures were homogenized at 10 000 r/min for 2 min. The freshly prepared emulsions were stored at ambient temperature for 7 days to evaluate their stability.

2.6 Morphological observation of SBCE

The microstructure of the prepared SBCE after storage at room temperature for 7 days was observed by optical microscope. Photomicrographs were captured using a digital camera and analyzed with image acquisition software (Phmia 2008 Cs ver. 2.3, Jiangxi Phoenix Optics Co., Ltd., Shangrao, China)[15].

2.7 Determination of centrifugal stability of SBCE

To evaluate the centrifugal stability of SBCE, the emulsion was centrifuged at 4 000 × g for a 5 min duration. The microstructure of the emulsion before and after centrifugation was observed using an optical microscope, and micrographs were captured with a digital camera and image acquisition software (Phmias 2008 Cs ver.2.3, Jiangxi Phenix Optical Co., Shangrao, China)[16].

2.8 Determination of freeze-thaw stability of SBCE

The freshly prepared emulsion was transferred into flat-bottom glass bottles and frozen at −20 °C for 24 h, followed by thawing in an oven at 30 °C for 2 h. Each group underwent three freeze-thaw cycles. Subsequent to each cycle, optical microscopy was employed to observe the emulsion microstructure, and micrographs were captured through a digital camera combined with its corresponding software[17].

2.9 Determination of antifreeze activity

2.9.1 Sample pre-treatment

For antifreeze activity evaluation, SBCE with a 60% oil phase was selected for fish pretreatment before freezing-thawing, due to its superior stability. Fresh Pacific salmon was purchased from a commercial market, processed immediately, and transported to the laboratory on ice within 1 h. Samples were divided into the following groups: Con, freshly slaughtered fish as the blank control; NCon, sample stored in an aqueous solution (matched to the concentration of the solvent used in other groups) as the negative control; SBCE0.5, sample immersed in 60% oil-phase SBCE containing 0.5 mg/mL SBC; SBCE1.0, sample immersed in 60% oil-phase SBCE containing 1.0 mg/mL SBC; SBCE2.0, sample immersed in 60% oil-phase SBCE containing 2.0 mg/mL SBC; SBCE3.0, sample immersed in 60% oil-phase SBCE containing 3.0 mg/mL SBC; PCon, sample immersed in 4% (m/m) sucrose plus 4% (m/m) sorbitol as the positive control. All samples were frozen at −20 °C for 24 h and thawed at 4 °C for 12 h until the core temperature reached 0–4 °C. Each group underwent five freeze-thaw cycles.

2.9.2 Extraction of Pacific salmon myofibrillar proteins (MFP)

MFP from Pacific salmon was extracted according to the previous literature with minor modifications[18–19]. After thawing, the muscle tissue was cut into small fragments and combined with four volumes (g/mL) of phosphate buffered saline (PBS; 20 mmol/L, pH 7.0). This mixture was homogenized at a speed of 3 500 r/min, after which it was centrifuged at 4 500 × g for 15 min at 4 °C. For the resulting precipitate, the same experimental protocol was applied for two more successive cycles. Subsequently, the final precipitate was centrifuged under the same conditions as above—this time mixed with four times its volume (g/mL) of PBS (pH 6.7) supplemented with 0.6 mol/L NaCl and the resulting supernatant was collected. The protein content of the extracted MFP was quantified using a standard curve generated with BSA as the reference standard; these content measurements were performed via the biuret method[20].

2.10 Analysis of conformational changes of MFP

2.10.1 Fluorescence spectroscopy

MFP samples were prepared to a content of 0.1 mg/mL; and its emission spectrum was measured between 300 and 450 nm at an excitation wavelength of 295 nm using a Fluorog-3 fluorescence spectrophotometer (Horiba Jobin Yvon, France)[18].

2.10.2 Circular dichroism (CD)

MFP samples were analyzed using CD spectrometer. Following a standard protocol with slight adjustments, samples at a content of 0.2 mg/mL were scanned from 200 to 250 nm, using a PBS solution as the blank reference[21–22].

2.10.3 Determination of oxidation of MFP

2.10.3.1 Protein solubility

For MFP samples, their solubility was measured following the protocols reported in previous literature, with minor modifications applied thereto[23]. Briefly, MFP solutions (3 mg/mL) were centrifuged at 4 500 × g and 4 °C for 15 min, and protein content in the supernatant was determined using the biuret method. Solubility was expressed as the percentage of protein in the supernatant relative to the total protein content in the original MFP solution.

2.10.3.2 Total sulfhydryl content

The total sulfhydryl group content in MFP was determined by reagent kit (A063-2-1, Nanjing Jianjian Bioengineering Research Institute Co., Ltd., Nanjing, China).

2.10.3.3 Carbonyl content

Protein carbonyl content in MFP was quantified via a commercial assay kit (A087-1, Nanjing Jiancheng Bioengineering Research Institute Co., Ltd., Nanjing, China) following the manufacturer's prescribed protocols.

2.10.3.4 Dityrosine content

For MFP samples, dityrosine content was assayed by a fluorescence spectrophotometer following the methods reported in previous literature[24]. MFP samples from each group were diluted to 1 mg/mL. Fluorescence intensity was recorded at an emission wavelength of 420 nm following excitation at 325 nm, and results are expressed in arbitrary fluorescence units (AU).

2.10.3.5 Ca^{2+}-ATPase activity

The Ca^{2+}-ATPase activity of MFP was measured using an ultratrace test kit (A070-3, Nanjing Jiancheng Bioengineering Institute Co., Ltd., Nanjing, China). MFP solutions (1 mg/mL) were analyzed according to the manufacturer's instructions.

2.11 Statistical analysis

All experiments were run with at least three replicate measurements, and corresponding statistical analysis was conducted by means of SPSS 26 (SPSS Inc., Chicago, USA). Intergroup differences were evaluated via one-way analysis of variance, where $P < 0.05$ was regarded as statistically significant.

3 Results and discussion

3.1 SDS-PAGE

Figure 1 shows the SDS-PAGE bands of SBC. The main band consists of α_1 chain, α_2 chain, and high molecular weight components, especially β component and a small amount of γ component, are also observed. In higher vertebrates, type I collagen is widely considered to be the major collagen found in most organs and was the first collagen to be identified[25], showed that SBCs from bone are mainly composed of type I collagen, a heterotrimer containing two identical α_1 chains and one α_2 chain. Similar electrophoretic protein patterns were found in collagen from the skin of the long-finned catfish (*Mystus macropterus*)[26]. Pepsin cleaves the cross-links containing telopeptides, and the β chain is simultaneously converted into two α chains[27]. A small amount of β component and a small amount of γ component were observed in SBC, which may be attributed to being cleaved by pepsin and converted into α component and other lower molecular weight components.

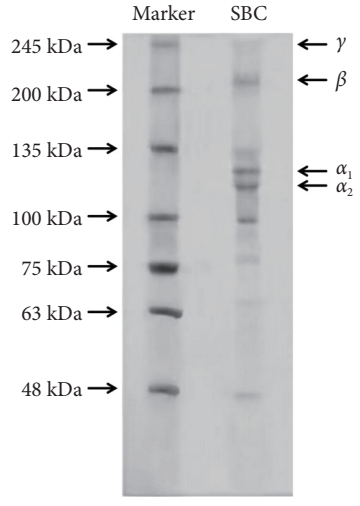

Figure 1 The effect of SBC on the SDS-PAGE pattern of frozen thawed Pacific salmon.

3.2 Textural properties and microstructure

3.2.1 Analysis of textural properties

Texture analysis results are shown in Table 1. Compared with the NCon and PCon groups, all SBC treated samples showed higher hardness, adhesiveness, and chewiness. Repeated freeze-thaw cycles induced ice crystal formation and growth, which disrupted cell membranes and accelerated protein and organelle damage, collectively softening muscle texture[28–29]. The hardness of the SBC0.5, SBC1.0, SBC2.0 and SBC3.0 groups were 54.12, 57.13, 61.14 and 57.38 g, respectively. The results showed, the SBC2.0 group exhibited higher hardness, adhesiveness, and chewiness, which may be attributed to its ability to limit ice crystal growth and thereby reduce ice crystal-induced muscle damage[30].

Table 1 The effects of SBC and SBCE on the textural characteristics of freeze-thawed Pacific salmon.

Samples		Hardness (g)	Springiness (mm)	Cohesiveness (g·s)	Adhesiveness (g)	Chewiness (mJ)	Resilience (mm)
	Con	65.63 ± 1.47^{a}	0.94 ± 0.02^{a}	3.58 ± 0.03^{a}	27.04 ± 0.83^{a}	25.77 ± 1.02^{a}	0.35 ± 0.01^{a}
	NCon	46.42 ± 1.89^{e}	0.83 ± 0.02^{d}	3.30 ± 0.04^{d}	17.64 ± 0.26^{f}	17.15 ± 0.13^{e}	0.23 ± 0.01^{e}
	PCon	51.95 ± 1.39^{d}	0.86 ± 0.03^{c}	3.42 ± 0.02^{c}	19.79 ± 0.71^{e}	19.61 ± 0.10^{d}	0.27 ± 0.01^{d}
SBC	SBC0.5	54.12 ± 1.11^{cd}	0.87 ± 0.02^{bc}	3.45 ± 0.03^{bc}	21.15 ± 1.06^{de}	20.65 ± 1.27^{cd}	0.29 ± 0.04^{cd}
	SBC1.0	57.13 ± 0.65^{c}	0.89 ± 0.02^{bc}	3.48 ± 0.03^{bc}	22.19 ± 0.43^{cd}	21.29 ± 0.64^{bcd}	0.28 ± 0.01^{cd}
	SBC2.0	61.14 ± 0.73^{b}	0.90 ± 0.01^{b}	3.52 ± 0.02^{ab}	24.53 ± 0.82^{b}	23.16 ± 0.89^{b}	0.32 ± 0.01^{b}
	SBC3.0	57.38 ± 0.41^{c}	0.88 ± 0.01^{bc}	3.49 ± 0.03^{bc}	24.14 ± 0.44^{bc}	22.86 ± 0.54^{bc}	0.30 ± 0.02^{bc}
	Con	66.66 ± 1.76^{a}	0.95 ± 0.02^{a}	3.61 ± 0.04^{a}	27.57 ± 0.99^{a}	25.84 ± 1.10^{a}	0.36 ± 0.01^{a}
	NCon	47.03 ± 1.67^{e}	0.84 ± 0.01^{d}	3.31 ± 0.04^{d}	17.46 ± 0.47^{f}	17.08 ± 0.18^{d}	0.24 ± 0.02^{d}
	PCon	53.16 ± 0.81^{d}	0.88 ± 0.01^{c}	3.44 ± 0.03^{c}	19.82 ± 0.60^{e}	19.67 ± 0.23^{c}	0.27 ± 0.02^{c}
SBCE	SBCE0.5	53.61 ± 1.18^{cd}	0.88 ± 0.02^{c}	3.45 ± 0.04^{c}	21.19 ± 1.17^{de}	20.80 ± 0.90^{c}	0.28 ± 0.03^{bc}
	SBCE1.0	58.02 ± 0.86^{c}	0.89 ± 0.01^{bc}	3.49 ± 0.04^{bc}	22.23 ± 0.45^{cd}	21.31 ± 0.55^{bc}	0.29 ± 0.02^{bc}
	SBCE2.0	61.55 ± 0.45^{b}	0.91 ± 0.01^{b}	3.53 ± 0.03^{b}	24.51 ± 0.33^{b}	22.90 ± 0.50^{b}	0.31 ± 0.01^{b}
	SBCE3.0	58.32 ± 0.39^{c}	0.90 ± 0.01^{bc}	3.50 ± 0.03^{bc}	24.04 ± 0.81^{bc}	22.70 ± 0.56^{b}	0.30 ± 0.01^{bc}

Note: Different lowercase letters in the same column indicate significant differences ($P < 0.05$).

3.2.2 Analysis of microstructure

As shown in Figure 2, the surface of fresh Pacific salmon (Con group) showed a regular aggregation structure, with tightly connected muscle fiber bundle structures and small tissue gaps. However, the gaps between fiber bundles in the NCon group were larger and the surface tears were severe. Loss of muscle tissue integrity and dense structure. Compared with the NCon group, the muscle fiber structure of the fish fillets in the SBC-added group was significantly better, which was consistent with the trends of moisture loss rate and texture damage. These results further confirmed the microstructural damage. This may be attributed to the fact that the addition of SBC regulates the growth of ice crystals and forms smaller ice crystals, thereby reducing damage to the cell membrane and having a good cryoprotective effect on Pacific salmon myofibrils[31]. From the SBC0.5 group and SBC1.0 group to the SBC2.0 group, a trend of reduced muscle tissue tears and smaller tissue gaps was observed, which indicates that the SBC2.0 group has a better tissue structure and has a better protective effect on the fish muscle tissue.

3.3 Analysis of changes in properties

3.3.1 Analysis of moisture loss

The changes in water holding capacity of Pacific salmon after five consecutive freeze-thaw cycles are shown in Table 2. After temperature fluctuations, the NCon group exhibited significant greater thawing and centrifugation loss rates compared to the Con group. This outcome is primarily attributed to ice crystal formation during the freezing process, which disrupted muscle fibers and diminished the water retention capability of the tissue[32]. SBC treatment reduced thawing, cooking, and centrifugation loss rates after repeated freeze-thaw cycles. Among all treatments, the SBC2.0 group showed the lowest thawing, cooking, and centrifugation loss rates. Thawing loss rate in the SBC3.0, SBC2.0, and SBC1.0 groups was 9.79%, 11.89%, and 8.97% lower than that in the NCon group, respectively. Centrifugation loss rate showed a similar pattern, with SBC2.0 showing the greatest reduction. These results suggest that SBC may suppress ice crystal growth during freeze-thaw cycles, thereby reducing muscle fiber damage and preserving water-holding capacity. Moisture loss during repeated freezing and thawing is often associated with lipid oxidation, protein aggregation and denaturation, and cell membrane disruption[33].

3.3.2 Analysis of color

During freeze-thaw cycles, protein denaturation and lipid oxidation generally increase b^*, whereas oxidation of pigments such as astaxanthin decreases a^*, leading to fading of the red color in fish[34]. The L^* mainly reflects moisture status and microstructural integrity of muscle, whereas a^* and b^* are associated with pigment retention and lipid oxidation, respectively. As shown in Table 2, among the

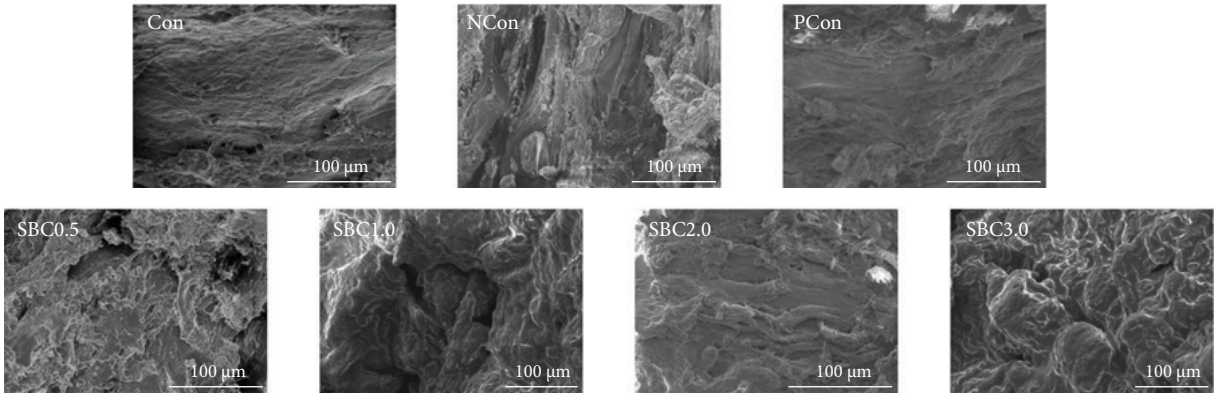

Figure 2 The effect of SBC on the microstructure of frozen thawed Pacific salmon.

Table 2 The effects of SBC and SBCE on color difference and moisture loss of Pacific salmon after freezing and thawing.

Samples		L^*	a^*	b^*	Thawing loss rate (%)	Cooking loss rate (%)	Centrifugal loss rate (%)
	Con	71.76 ± 0.25^{a}	17.74 ± 0.59^{a}	25.56 ± 0.30^{e}		11.86 ± 2.98^{f}	14.06 ± 2.39^{e}
	NCon	58.83 ± 0.25^{e}	11.59 ± 0.31^{e}	31.84 ± 0.35^{a}	20.11 ± 5.08^{a}	25.33 ± 5.81^{a}	33.86 ± 5.41^{a}
	PCon	65.43 ± 0.55^{d}	13.31 ± 0.11^{d}	28.64 ± 0.09^{b}	15.63 ± 2.89^{b}	21.21 ± 5.65^{b}	28.99 ± 5.91^{b}
SBC	SBC0.5	66.23 ± 0.94^{cd}	14.17 ± 0.15^{cd}	27.63 ± 0.73^{bcd}	13.89 ± 3.47^{c}	19.65 ± 4.97^{bc}	25.57 ± 5.44^{bc}
	SBC1.0	67.06 ± 0.65^{c}	14.99 ± 0.14^{bc}	27.50 ± 0.28^{cd}	11.14 ± 2.05^{d}	17.47 ± 2.50^{cd}	23.36 ± 7.11^{cd}
	SBC2.0	68.91 ± 0.66^{b}	15.97 ± 0.28^{b}	26.65 ± 0.13^{d}	8.22 ± 2.46^{e}	14.63 ± 2.03^{e}	19.60 ± 4.29^{d}
	SBC3.0	66.57 ± 0.19^{cd}	15.35 ± 0.63^{b}	27.97 ± 0.37^{bc}	10.32 ± 2.71^{d}	17.00 ± 2.51^{d}	22.27 ± 7.00^{cd}
	Con	74.49 ± 0.55^{a}	18.62 ± 0.30^{a}	20.96 ± 0.39^{e}		9.91 ± 0.36^{f}	9.24 ± 0.78^{d}
	NCon	58.71 ± 0.41^{e}	11.55 ± 0.64^{e}	30.58 ± 0.61^{a}	25.31 ± 1.01^{a}	24.16 ± 1.22^{a}	18.29 ± 1.11^{a}
	PCon	64.48 ± 0.66^{d}	14.10 ± 0.39^{d}	27.17 ± 0.38^{b}	18.55 ± 0.97^{b}	17.29 ± 0.52^{bc}	14.85 ± 0.40^{b}
SBCE	SBCE0.5	64.55 ± 0.92^{d}	14.50 ± 0.19^{d}	26.56 ± 0.49^{b}	18.18 ± 0.89^{b}	18.09 ± 0.84^{b}	14.77 ± 0.44^{b}
	SBCE1.0	67.09 ± 0.37^{c}	16.10 ± 0.22^{bc}	24.73 ± 0.15^{c}	14.82 ± 0.20^{c}	14.26 ± 0.54^{de}	13.12 ± 0.35^{bc}
	SBCE2.0	69.81 ± 0.33^{b}	16.61 ± 0.14^{b}	23.11 ± 0.18^{d}	10.38 ± 0.54^{d}	13.17 ± 0.37^{e}	12.13 ± 0.47^{c}
	SBCE3.0	67.73 ± 0.21^{c}	15.62 ± 0.06^{c}	24.51 ± 0.19^{c}	13.81 ± 1.03^{c}	15.39 ± 0.93^{cd}	12.67 ± 0.58^{c}

Note: Different lowercase letters in the same column indicate significant differences ($P < 0.05$).

treated groups, the SBC2.0 group showed a lower L^* than the Con group, but a significantly higher L^* than the NCon and PCon groups ($P < 0.05$). The b^* of SBC2.0 was significantly lower than those of NCon and PCon ($P < 0.05$). The a^* of the treatment group, SBC0.5, SBC1.0 and SBC3.0 are less than SBC2.0. In general, the addition of SBC protected the color changes of fish meat, and the SBC2.0 group had the best protection effect.

3.4 E-nose analysis

The results of E-nose analysis are shown in Figure 3. In fish, alcohols generally form through processes like the reduction of sugaramino acid complexes and aldehydes, along with the enzymatic oxidation of fatty acids[35]. The W2S sensor detected the volatile compounds associated with fishy odor, mainly including aldehydes, ketones, and alcohols. The NCon group showed the strongest responses for sulfides (W1W and W2W) and alcohols (W2S). Among all treated groups (excluding the fresh Con group), SBC2.0 showed the smallest change in W2S response, indicating relatively less odor formation after the freeze-thaw cycle. This may be attributed to inhibited protein denaturation and lipid oxidation induced by SBC.

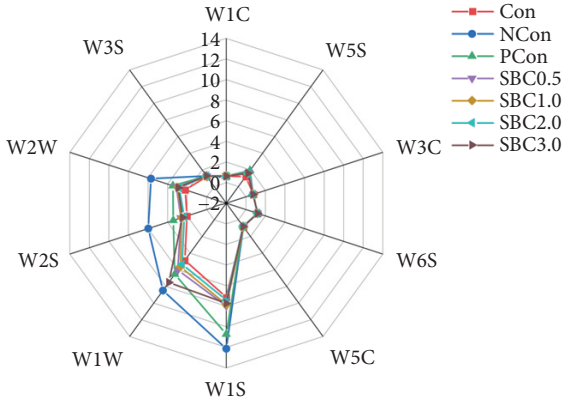

Figure 3 The effect of SBC on the E-nose response of frozen thawed Pacific salmon.

3.5 Stability analysis of emulsion

3.5.1 Storage stability

During storage, the emulsion separated into the upper layer of emulsion and the lower layer of clear liquid (Figure 4A). However, demulsification or oil precipitation was not observed after 7 days of room-temperature storage. Microscopy images (Figure 4B) showed that droplet size increased in emulsions with lower oil-phase fractions (10%–50%), while only minor changes were observed in emulsions with higher oil-phase fractions (60%–70%). The results show that the 60% and 70% oil phase volume emulsions have no obvious changes after being stored at room temperature for 7 days, and have the best stability. Similarly, related studies also reported that emulsions with an oil fraction below 60% showed pronounced droplet growth during storage, whereas those containing 60%–70% oil phase showed minimal changes in droplet size over time.

3.5.2 Centrifugal stability

As shown in Figure 5, emulsions with an oil-phase volume below 60% showed obvious foaming and phase separation. This instability may be attributed the insufficient oil phase for supporting SBC adsorption at the oil/water interface. Emulsions with low oil contents (10%–30%) exhibited broad droplet-size distributions with an increased proportion of large droplets, while those containing 60%–70% oil showed improved stability.

3.5.3 Freeze-thaw stability

During freeze-thaw cycling, droplet size gradually enlarged, accompanied by progressive emulsion destabilization manifested as emulsion breakdown and phase separation. This behavior may be attributed to volumetric fluctuations of ice crystals formed in the continuous phase during freezing and thawing, which induced localized mechanical stress, disrupt the interfacial film, and promote droplet coalescence[36]. As shown in Figure 6, after the first freeze-thaw cycle, emulsions containing 10%–50% oil phase showed a significant increase in droplet size. By the second cycle, these emulsions exhibited obvious foaming and phase separation, and demulsification

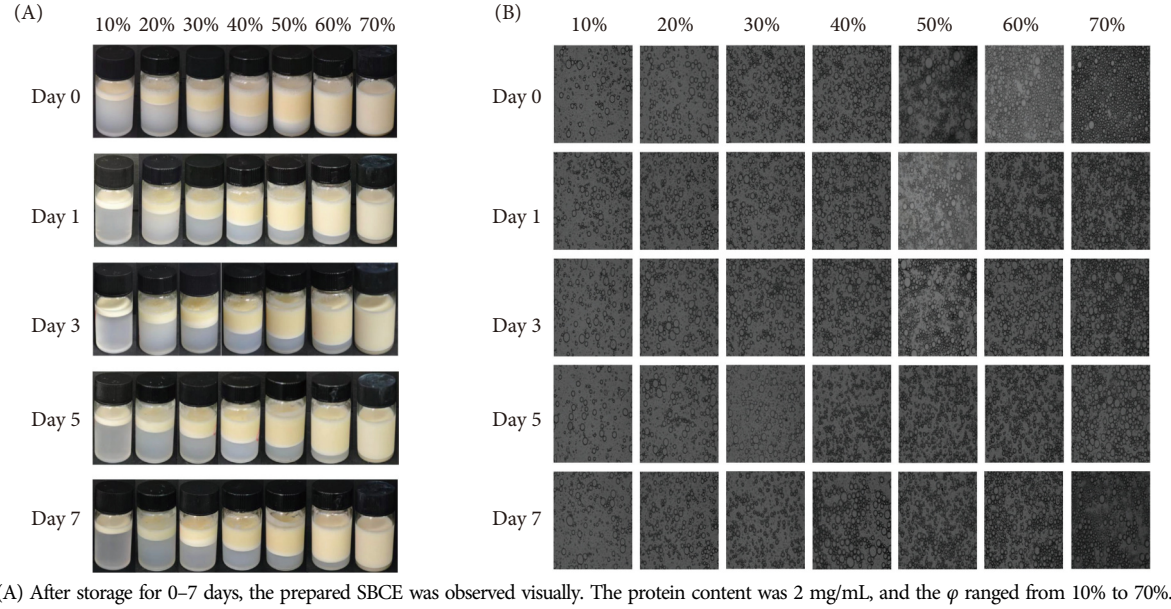

Figure 4 (A) After storage for 0–7 days, the prepared SBCE was observed visually. The protein content was 2 mg/mL, and the φ ranged from 10% to 70%. (B) After storage for 0–7 days, the microstructure of the prepared SBCE was observed under a microscope. The protein content was 2 mg/mL, and the φ ranged from 10% to 70%.

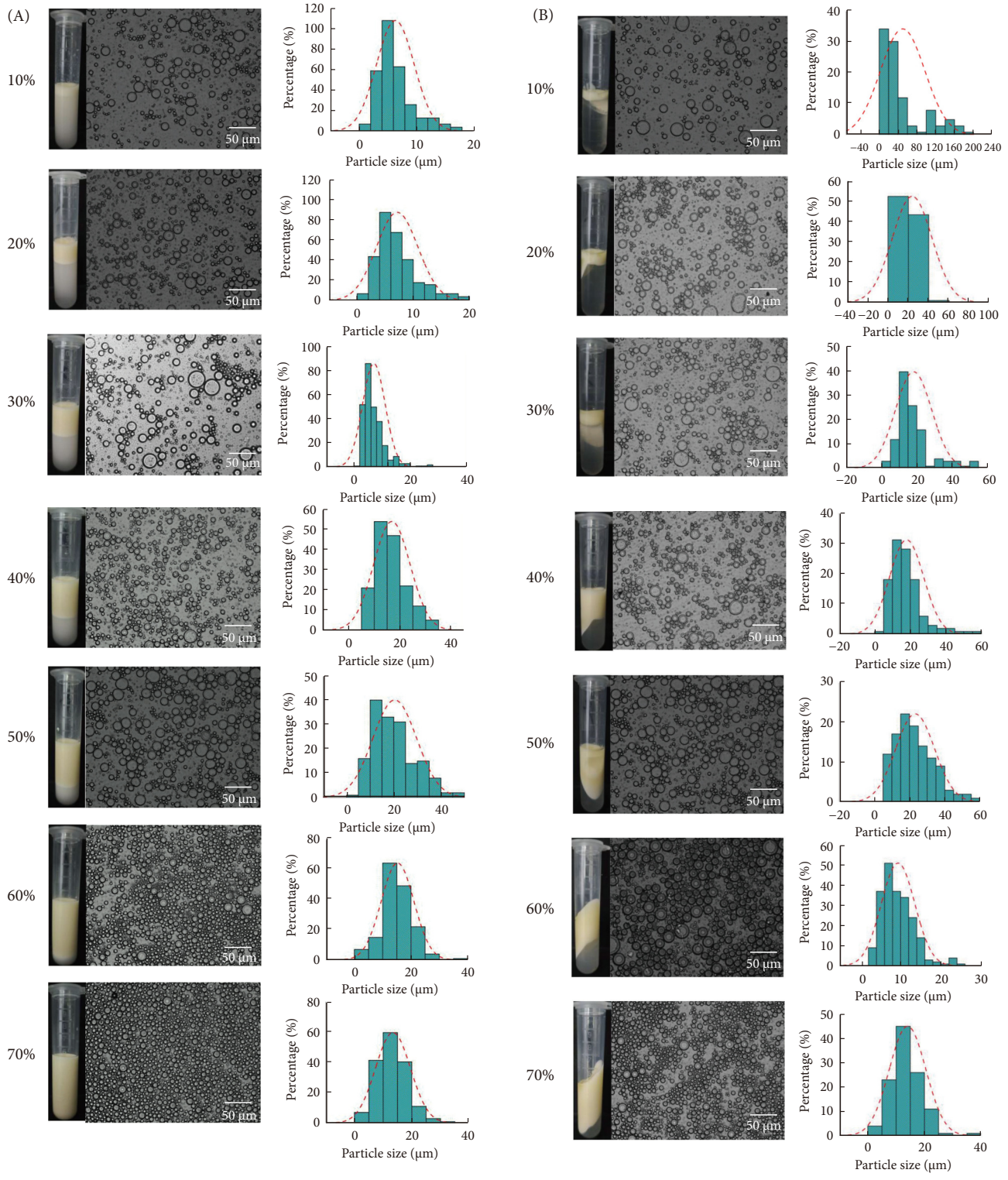

Figure 5 Photos and particle size microscopic images of SBC stabilizing detergent with a protein content of 2 mg/mL and φ ranged from 10% to 70%. (A) Non centrifuged, (B) centrifuge.

microstructures were observed under microscopy. For emulsions containing 60% and 70% oil phase, a significant increase in droplet size was observed only after the third freeze-thaw cycle, while neither foaming nor phase separation occurred.

Overall, although a slight increase in droplet size was detected in the emulsion with 60% and 70% oil content, no further macroscopic deterioration was observed. This suggests that emulsions with higher oil fractions (and higher particle concentrations) show stronger freeze-thaw stability than those with lower particle concentrations[37].

3.6 Analysis of texture properties

During the freeze-thaw cycle, the microscopic morphology and size of ice crystals are the core factors that determine the changes in the

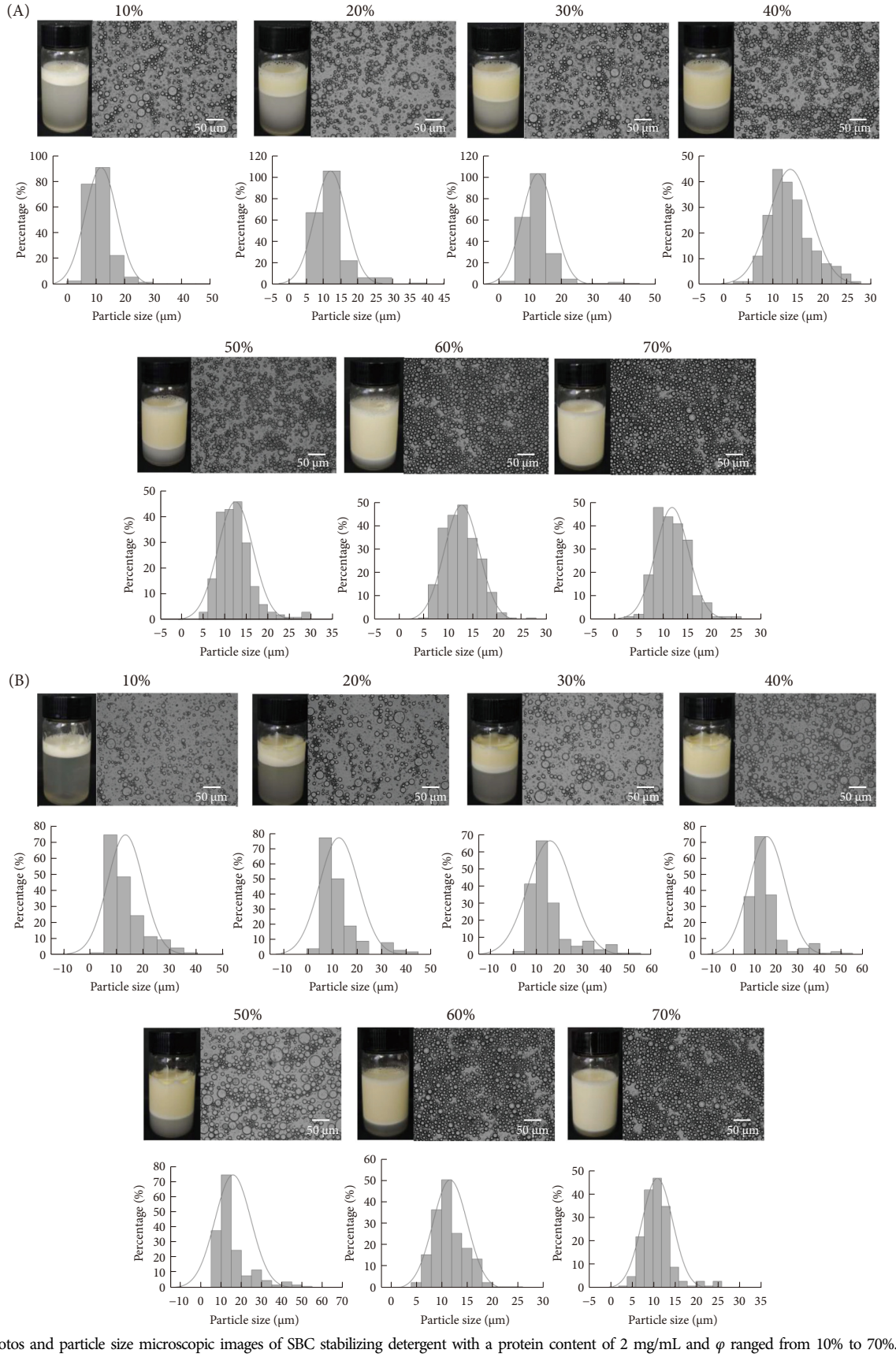

Figure 6 Photos and particle size microscopic images of SBC stabilizing detergent with a protein content of 2 mg/mL and φ ranged from 10% to 70%. (A) Before freeze-thaw; (B) first freeze-thaw cycle; (C) second freeze-thaw cycle; (D) third freeze-thaw cycle.

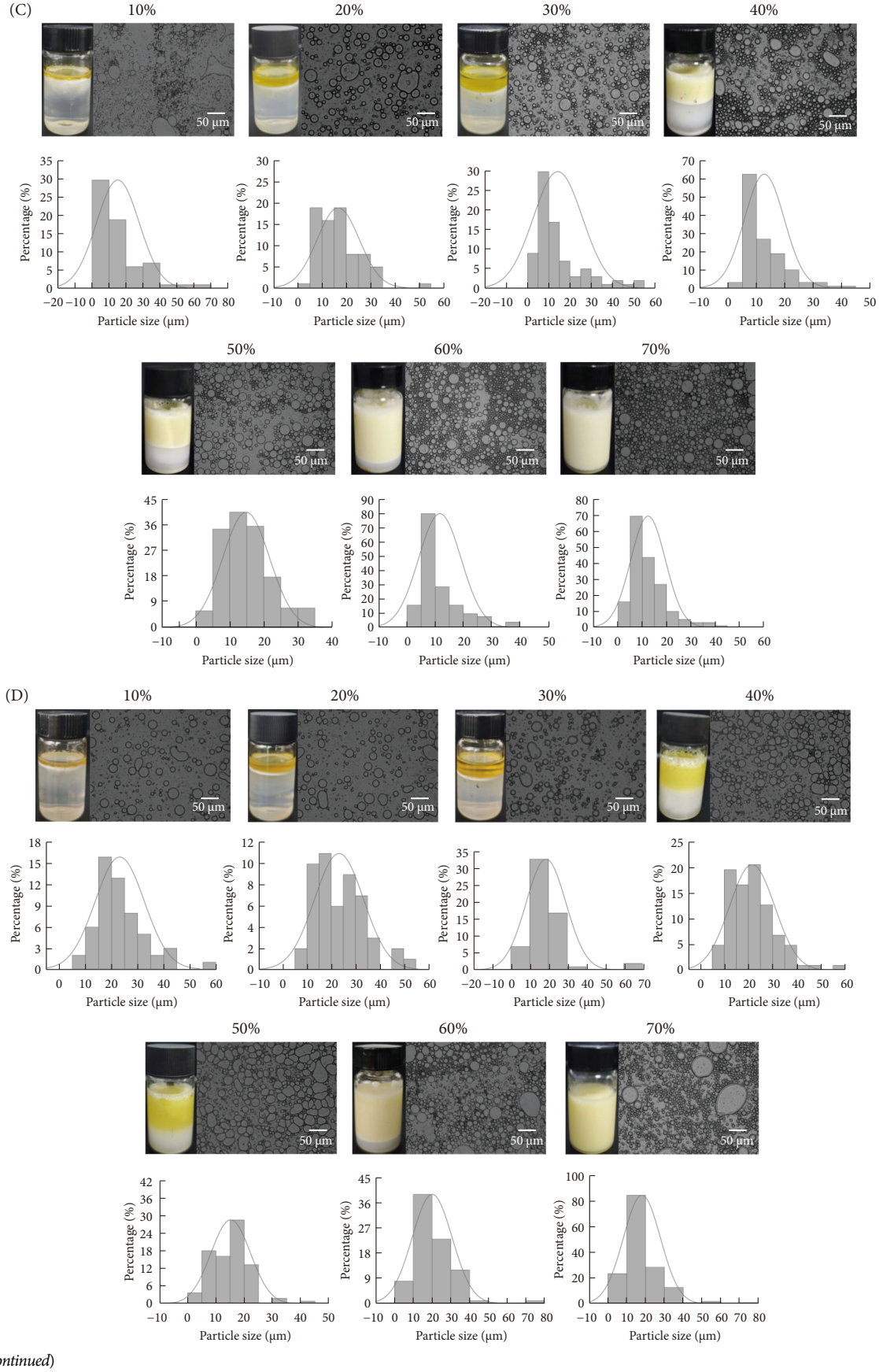

Figure 6 (*Continued*)

texture characteristics of fish meat. Fish meat without effective protection is prone to form ice crystals with larger sizes, irregular shapes and uneven distribution during repeated freezing and thawing. During the growth and recrystallization process, these ice crystals will produce strong mechanical puncture and squeezing effects on muscle fibers, directly causing cell membrane rupture, enlargement of intercellular spaces and dissociation of myofibrillar protein structure. The final manifestation is that the hardness, springiness and chewiness of fish meat are significantly reduced, the overall softening of muscle tissue and serious texture deterioration[28–29]. As shown in Table 1, after five freeze-thaw cycles, reductions in hardness, chewiness, and resilience were observed in the control group (Con), indicating significant textural deterioration. This deterioration was likely caused by ice-crystal-induced cellular rupture and protein structural damage, which weakened muscle fiber integrity and resulted in softer flesh. Compared with the NCon group, significantly higher hardness and springiness were observed in SBCE-treated samples ($P < 0.05$). Among all freeze-thaw-treated groups, the highest hardness and springiness values were obtained in the SBCE2.0 group, which were significantly higher than those in both the NCon and PCon groups ($P < 0.05$). This improvement may be attributed to hydrogen bonding between SBCE and the ice-crystal surface[30]. This interaction may limit ice crystal growth and reduce tissue damage during freeze-thaw cycling, contributing to improved texture retention after thawing.

3.7 Analysis of changes in properties

3.7.1 Analyses of moisture loss

Repeated freeze-thaw cycles induced pronounced structural disruption in salmon muscle, which intensified moisture loss and deteriorated quality. As shown in Table 2, a substantial moisture loss was observed in the NCon group, with thawing loss rate and cooking loss rate of 25.31% and 24.16%, respectively. This increase was attributed to freeze-thaw-induced mechanical damage to muscle cells, which reduced the ability of the tissue to retain water[38]. In contrast, water loss was significantly reduced after SBCE treatment. The SBCE2.0 group exhibited the lowest thawing loss rate (10.38%) and cooking loss rate (13.17%). This improvement indicated that SBCE alleviated protein denaturation and enhanced water retention during heating. A similar trend was observed for centrifugal loss rate, which characterizes the water-binding strength within muscle tissue. The centrifugal loss rate of the SBCE2.0 group was 12.13%, significantly lower than that of the NCon group (18.29%) ($P < 0.05$). This result suggested improved water-protein interactions and a strengthened MFP network, which reduced water separation during centrifugation.

3.7.2 Analysis of color

As summarized in Table 2, the Con group showed the highest L^* (74.49). After freeze-thaw cycling, a significant decrease in brightness was observed in the NCon group, with the L^* reduced to 58.71. After SBCE treatment, brightness was partially restored. The L^* increased to 69.81 in the SBCE2.0 group, which was significantly higher than those of the NCon and PCon groups ($P < 0.05$). For redness, the a^* in the NCon group decreased to 11.55 after repeated freeze-thaw cycles, indicating pigment loss and oxidation. This change in a^* during the freezing process may be attributed to the conversion of myoglobin to metmyoglobin and the oxidative degradation of heme pigments[32]. The b^* increased after freeze-thaw cycling, which was attributed to oxidative changes in lipid[39]. The lowest b^* was obtained in the SBCE2.0 group (23.11), which was significantly lower than that of the NCon (30.58) and PCon (27.17) groups ($P < 0.05$). SBCE effectively protected the muscle fiber structure, which in turn reduced tissue damage caused by ice crystals. This led to the retention of favorable light reflection properties, enhanced brightness, and better preservation of muscle color throughout freeze-thaw cycles. In summary, among all treatments, the best performance was observed in the SBCE2.0 group. SBCE significantly improved color stability during freeze-thaw cycling.

3.8 E-nose analysis

Volatile compounds released from spoiled fish mainly include aldehydes, ketones, unsaturated alcohols, and inorganic sulfides[40–41]. As shown in Figure 7, among the ten sensors, W1W (inorganic sulfide), W1S (aromatic components) and W2S (alcohols) have the highest responsiveness. Among the three sensors, the response of the NCon group was the most obvious, indicating that high concentrations of sulfides, alcohols, and other compounds that cause bad odors are formed during the freeze-thaw cycle, while the sensor response value dropped significantly after SBCE treatment. Among all freeze-thaw-treated groups, the lowest W2S response was obtained in the SBCE2.0 group. These results suggested that SBCE suppressed the generation of undesirable volatile compounds during freeze-thaw cycling.

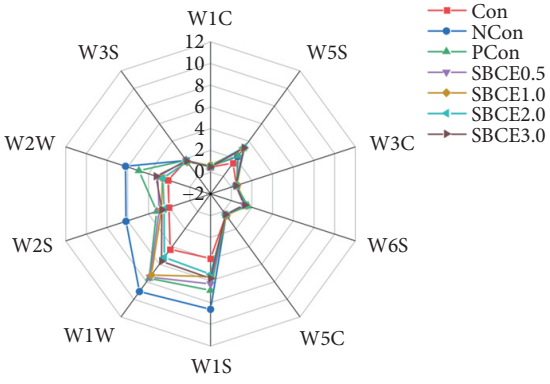

Figure 7 The effect of SBCE on the E-nose response of frozen thawed Pacific salmon.

3.9 Analysis of MFP conformational changes

3.9.1 Fluorescence spectroscopy analysis

Endogenous fluorescence is used to evaluate alterations in tryptophan residues and the degree of protein oxidation due to changes in tryptophan fluorescence[42–43]. As shown in Figure 8A, during freeze-thaw cycling, tryptophan residues were exposed to a more polar microenvironment, which may be attributed to protein unfolding and increased surface hydrophobicity. Compared with the NCon group, a less obvious shift in λ_{max} and a higher fluorescence intensity were observed in the SBCE2.0 group. The lower fluorescence intensity observed after repeated freeze-thaw cycles was attributed to tryptophan exposure induced by protein aggregation, as well as ice-crystal-induced tissue disruption that

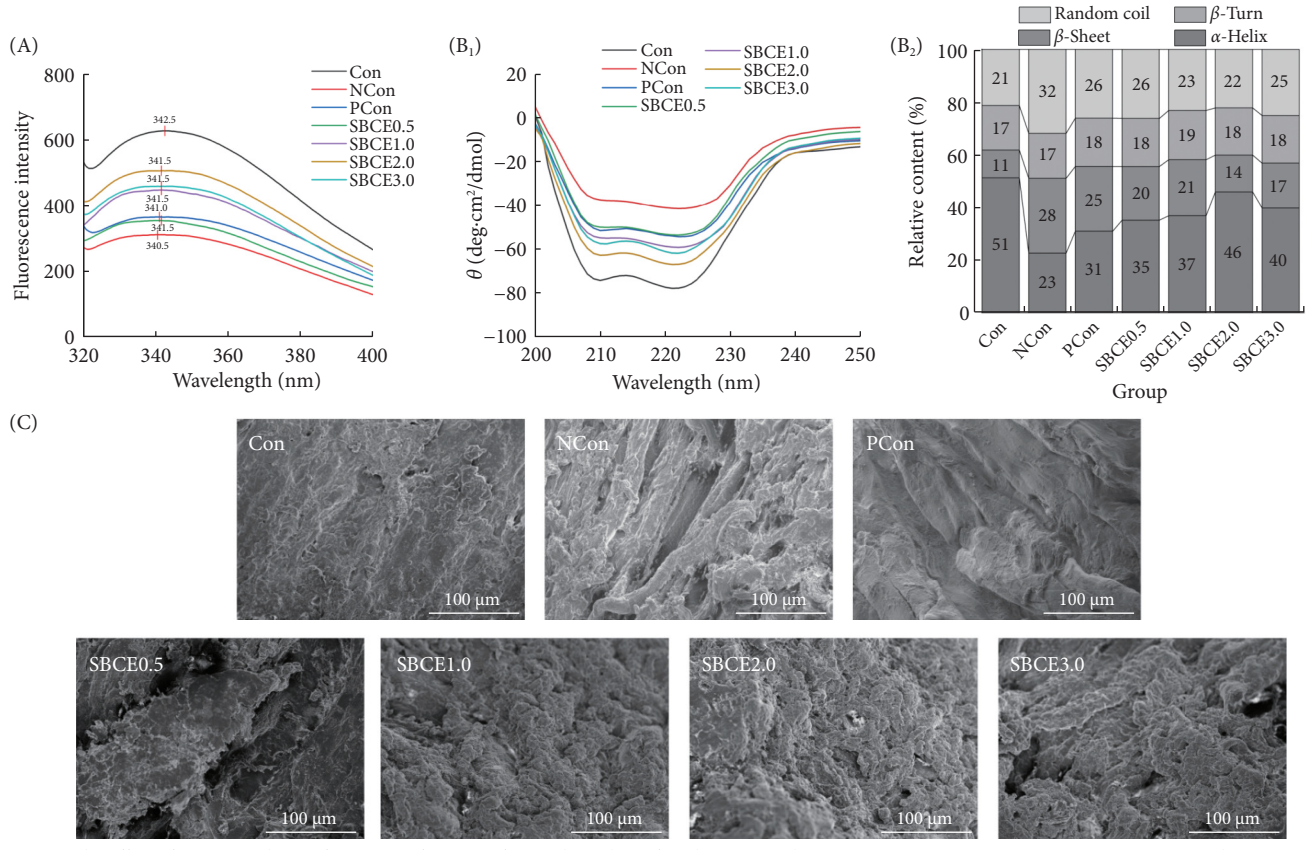

Figure 8 The effect of SBCE on the conformation of MFP in frozen thawed Pacific salmon. (A) Fluorescence spectrum; (B_1) CD spectrum; (B_2) secondary structure relative content; and (C) SEM images of Pacific salmon (400×).

promoted protein oxidation. Overall, SBCE alleviated freeze-thaw-induced conformational changes of MFP proteins and reduced protein denaturation.

3.9.2 CD analysis

CD spectroscopy is used to evaluate protein secondary structure based on conformational changes in the peptide backbone[44–45]. The CD spectra (Figure 8B_1) showed two characteristic negative bands at 210 and 222 nm in all groups, indicating the presence of α-helix structures in MFP. A reduced peak intensity was observed after SBCE treatment. The α-helix is the dominant secondary structure in MFP, its disruption during freeze-thaw cycling resulted in conversion to β-sheet and random coil. The NCon group showed increased β-sheet and random coil relative contents and a higher α-helix relative content was observed in the SBCE2.0 group than in the NCon group (Figure 8B_2). This conversion may be attributed to the growth of ice crystals and recrystallization, which promoted protein aggregation and exposed hydrophobic residues, thereby increasing β-sheet and random coil relative contents. Overall, SBCE alleviated secondary-structure disruption induced by freeze-thaw cycling and improved conformational stability of MFP at low temperature.

3.9.3 Analysis of microstructure

As presented in Figure 8C, a compact and continuous myofiber network with small inter-fiber gaps was observed in the Con group, indicating intact muscle integrity. In contrast, enlarged gaps between fiber bundles and pronounced surface discontinuities were observed in the NCon group, indicating severe structural disruption. This microstructural damage was supported by the highest moisture loss in the NCon group (Table 2) and the strongest protein denaturation (Figures 6 and 7). These results indicated that freezing process promoted the formation and growth of ice crystals, which disrupted cell membranes and loosened the muscle structure, in agreement with previous reports[46].

After freeze-thaw cycling, surface roughness and crack formation were observed on the muscle tissue of the NCon group. Such structural impairment stemmed from ice crystal formation between muscle fibers, which in turn disrupted fiber bundles and triggered dehydration under the osmotic pressure exerted by the concentrated unfrozen phase. In contrast, SBCE treatment mitigated tissue disruption and preserved a more compact muscle fiber structure. This protective effect may stem from that SBCE inhibited the growth of large ice crystals and alleviated water loss and muscle texture deterioration.

3.10 MFP oxidation analysis

3.10.1 Protein solubility

The solubility of MFP is presented in Figure 9A. Higher protein solubility was observed in all SBCE-treated groups than in the NCon group. Compared with the Con group, protein solubility was increased by 8.90%, 14.24%, 19.48%, and 13.05% in the SBCE0.5, SBCE1.0, SBCE2.0, and SBCE3.0 groups, respectively. SBCE2.0 group showed the highest solubility among all frozen samples, indicating its efficiency on maintaining protein solubility. Solubility loss is probably due to protein oxidation arising from the repeated conversion of the aqueous phase during freeze-thaw cycles[47–48].

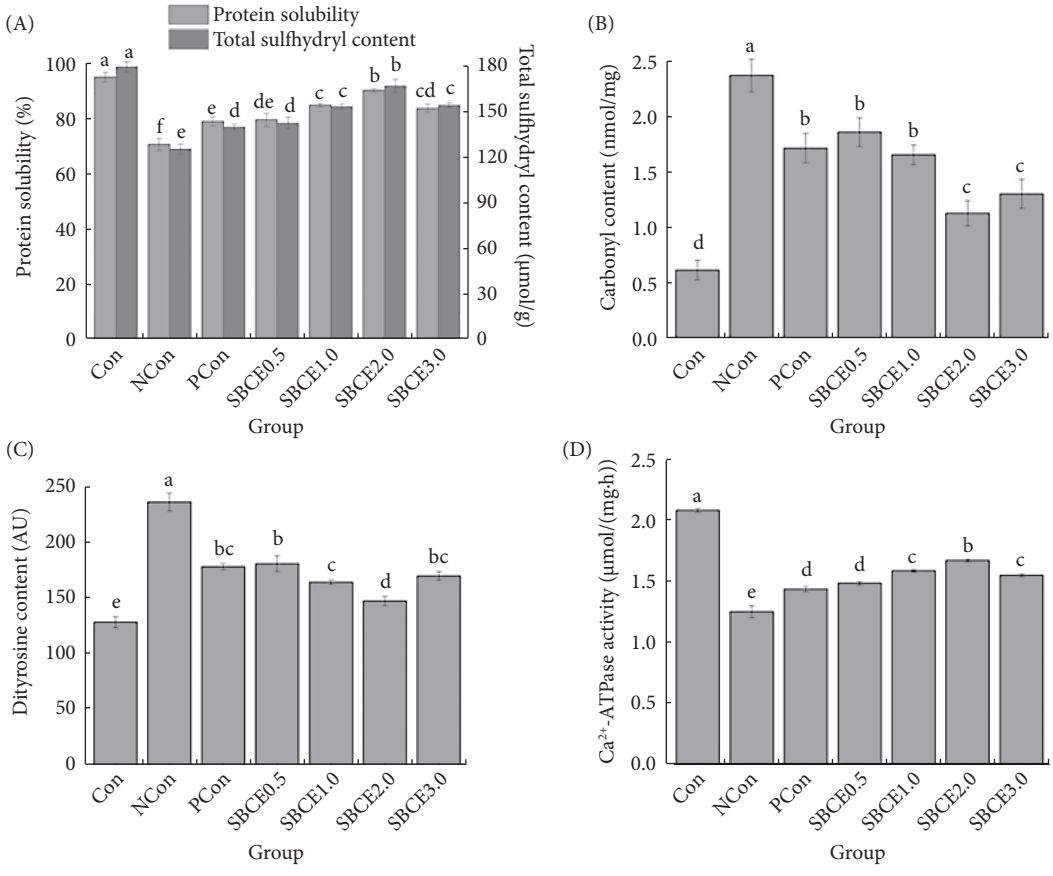

Figure 9 The effect of SBCE on the aggregation and oxidation of MFP in frozen thawed Pacific salmon. (A) Protein solubility and total sulfhydryl content, (B) carbonyl content, (C) dityrosine content, (D) Ca^{2+}-ATPase activity. Different lowercase letters indicate significant differences ($P < 0.05$).

3.10.2 *Total sulfhydryl content*

Total thiol groups are important for maintaining protein structure and functionality. The oxidation degree of total thiol groups is commonly used as an indicator of protein oxidation[49]. After five freeze-thaw cycles, total sulfhydryl content in Pacific salmon muscle was reduced, indicating enhanced MFP oxidation (Figure 9A). The highest total sulfhydryl content was observed in the Con group (without freeze-thaw cycling), while the lowest was observed in the NCon group soaked in water. Compared with the Con group, the total sulfhydryl contents of the NCon, PCon, SBCE0.5, SBCE1.0, SBCE2.0, and SBCE3.0 groups were reduced by 54.05, 39.64, 36.94, 26.13, 12.61, and 25.23 μmol/g, respectively. This reduction was mainly attributed to the oxidation of thiol groups into disulfide bonds and the formation of sulfonic acid products[50]. Among all treatments, SBCE2.0 retained the highest thiol content. The addition of SBCE effectively prevented myofibril degeneration, which may be attributed to the reduction recrystallization during freezing.

3.10.3 *Carbonyl content*

Protein carbonyl content is widely used as an indicator of protein oxidation[51]. As shown in Figure 9B, the Con group, which did not experience freeze-thaw cycles, exhibited the lowest carbonyl level. Compared with the NCon group, the carbonyl contents of the PCon, SBCE0.5, SBCE1.0, and SBCE3.0 groups were reduced by 0.65, 0.51, 0.72, and 1.07 nmol/mg, respectively. The greatest reduction (1.13 nmol/mg) was observed in the SBCE2.0 group. These results suggest that SBCE treatment (especially SBCE2.0) reduced cell deformation and rupture during freezing, indicating improved freezing stability.

3.10.4 *Dityrosine content*

Dityrosine is a cross linked amino acid residue that may undergo oxidation to form tyrosylphenoxy[51–52]. As presented in Figure 9C, fresh fish (Con) showed the lowest level of dimeric tyrosine, while elevated contents of dimeric tyrosine were identified in the NCon group after freeze-thaw cycles. This may be ascribed to the disruption of fish tissue structure by ice crystals, which induced enhanced protein oxidation. Among all experimental treatments, the SBCE2.0 group had the lowest content of dimeric tyrosine. These results indicate that SBCE effectively suppressed protein oxidation and cross linking, which in turn preserved muscle structural integrity during freezing.

3.10.5 *Ca^{2+}-ATPase activity*

Ca^{2+}-ATPase activity is commonly used as an indicator of myosin head integrity and the denaturation extent of this region[53]. As shown in Figure 9D, the lowest Ca^{2+}-ATPase activity was observed in the NCon group, indicating the greatest loss of myosin head integrity after freeze-thaw cycling. In the Con group, Ca^{2+}-ATPase activity was 2.07 μmol/(mg·h). The corresponding enzyme activities in the NCon, PCon, SBCE0.5, SBCE1.0, SBCE2.0, and SBCE3.0 groups were measured as 1.24, 1.43, 1.48, 1.58, 1.67, and 1.54 μmol/(mg·h), respectively. Enzyme activity in the SBCE2.0 group was significantly higher than in all other treatment groups ($P < 0.05$). These results indicate that the addition of SBCE can reduce muscle fiber damage, prevent protein oxidation, and maintain Ca^{2+}-ATPase activity, thus protecting MFP from freeze denaturation.

4 Conclusion

In this study, SBCEs were successfully prepared and showed effective protective effect on fish during freeze-thaw cycles. Stability tests at room temperature, freeze-thaw processes, and during centrifugation showed that the emulsion with an oil phase volume of 60%–70% showed the best stability. According to the results from texture, moisture loss, and E-nose analysis, the SBCE treatment effectively enhanced the water holding capacity of the fish samples. SBCE mitigated the quality deterioration and odor alterations induced by ice crystals. This study showed that SBC is a promising stabilizer for O/W emulsions, and the resulting SBCE provides significant cryoprotective effects on Pacific salmon during freeze-thaw cycles. The findings from this study supports the development of edible antifreeze emulsions for potential food applications.

Conflict of interest

The authors declare no conflicts of interest.

Acknowledgments

This work was funded by Open Foundation of Dalian Xinghai Bay Laboratory (Dljswgj202405).

Data availability

Data will be made available on request.

Author contributions

Zhe Xu: Writing-review & editing, writing-original draft, methodology, investigation, funding acquisition, formal analysis. Yikun Xu: Writing-review & editing, writing-original draft, methodology, investigation, formal analysis. Xuguang Mo: Conceptualization, methodology, conceptualization. Ziyu Zhang: Software, methodology. Haoran Wu: Software, methodology, conceptualization. Yidi Luo: Software, methodology, conceptualization. Tingting Li: Writing-review & editing, writing-original draft, methodology, funding acquisition, conceptualization.

References

[1] X. Chen, J. Wu, X. Cai, et al., Production, structure-function relationships, mechanisms, and applications of antifreeze peptides, Compr. Rev. Food Sci. F. 20 (2021) 542–562. https://doi.org/10.1111/1541-4337.12655.

[2] R. Banerjee, N. B. Maheswarappa, Superchilling of muscle foods: potential alternative for chilling and freezing, Crit. Rev. Food Sci. 59 (2019) 1256–1263. https://doi.org/10.1080/10408398.2017.1401975.

[3] L. Du, M. Betti, Chicken collagen hydrolysate cryoprotection of natural actomyosin: mechanism studies during freeze-thaw cycles and simulated digestion, Food Chem. 211 (2016) 791–802. https://doi.org/10.1016/j.foodchem.2016.05.092.

[4] X. Chen, J. Wu, X. Li, et al., Investigation of the cryoprotective mechanism and effect on quality characteristics of surimi during freezing storage by antifreeze peptides, Food Chem. 371 (2022) 131054. https://doi.org/10.1016/j.foodchem.2021.131054.

[5] H. C. Moghadas, J. S. Smith, R. Tahergorabi, Recent advances in the application of edible coatings for shelf-life extension of strawberries: a review, Food Bioprocess Tech. 18 (2025) 1079–1103. https://doi.org/10.1007/s11947-024-03517-7.

[6] X. Chen, X. Shi, X. Cai, et al., Ice-binding proteins: a remarkable ice crystal regulator for frozen foods, Crit. Rev. Food Sci. 61 (2021) 3436–3449. https://doi.org/10.1080/10408398.2020.1798354.

[7] Y. Wang, Y. Chen, Y. Li, et al., Collagen as a diversely structural biomaterial: from assembly strategies to potential applications in food industry, Food Hydrocoll. 159 (2025) 110694. https://doi.org/10.1016/j.foodhyd.2024.110694.

[8] W. Jiang, D. Cai, M. Wu, et al., Unraveling the cryoprotective molecular mechanisms of antifreeze peptides: new insights from simultaneous interactions with ice crystals and lactalbumin proteins, J. Agric. Food Chem. 73 (2025) 24427–24436. https://doi.org/10.1021/acs.jafc.5c08418.

[9] Ç. Dikel, Y. Yanar, Characterization of acid-soluble collagen from by-product bones of European sea bass (*Dicentrarchus labrax*) and common carp (*Cyprinus carpio*), Food Sci. Nutr. 13 (2025) e70059. https://doi.org/10.1002/fsn3.70059.

[10] S. Menéndez-Tasé, E. Gaeta-Leal, D. I. Téllez-Medina, et al., Native collagen and total lipid extract obtained from caranx hyppos by-products: characterization for potential use in the biomedical and nutraceutical fields, Mar. Drugs 23 (2025) 432. https://doi.org/10.3390/md23110432.

[11] W. Lan, X. Hu, X. Sun, et al., Effect of the number of freeze-thaw cycles number on the quality of Pacific white shrimp (*Litopenaeus vannamei*): an emphasis on moisture migration and microstructure by LF-NMR and SEM, Aquac. Fish. 5 (2020) 193–200. https://doi.org/10.1016/j.aaf.2019.05.007.

[12] X. Chen, X. Li, F. Yang, et al., Effects and mechanism of antifreeze peptides from silver carp scales on the freeze-thaw stability of frozen surimi, Food Chem. 396 (2022) 133717. https://doi.org/10.1016/j.foodchem.2022.133717.

[13] Q. Li, X. Sun, E. Mubango, et al., Effects of protein and lipid oxidation on the water holding capacity of different parts of bighead carp: eye, dorsal, belly and tail muscles, Food Chem. 423 (2023) 136238. https://doi.org/10.1016/j.foodchem.2023.136238.

[14] Y. Zhou, S. Lu, H. Chen, et al., Potential freezing resistance of collagen peptide-fish oil high internal phase emulsion: enhancing freeze-thaw stability of 3D-printed surimi, Food Hydrocoll. 172 (2026) 112001. https://doi.org/10.1016/j.foodhyd.2025.112001.

[15] X. S. Qin, Z. G. Luo, X. C. Peng, Fabrication and characterization of quinoa protein nanoparticle-stabilized food-grade Pickering emulsions with ultrasound treatment: interfacial adsorption/arrangement properties, J. Agric. Food Chem. 66 (2018) 4449–4457. https://doi.org/10.1021/acs.jafc.8b00225.

[16] Q. Zhu, Y. Li, S. Li, et al., Fabrication and characterization of acid soluble collagen stabilized Pickering emulsions, Food Hydrocoll. 106 (2020) 105875. https://doi.org/10.1016/j.foodhyd.2020.105875.

[17] W. Xu, Y. Jia, J. Li, et al., Pickering emulsion with high freeze-thaw stability stabilized by xanthan gum/lysozyme nanoparticles and konjac glucomannan, Int. J. Biol. Macromol. 261 (2024) 129740. https://doi.org/10.1016/j.ijbiomac.2024.129740.

[18] M. Cao, A. Cao, J. Wang, et al., Effect of magnetic nanoparticles plus microwave or far-infrared thawing on protein conformation changes and moisture migration of red seabream (*Pagrus major*) fillets, Food Chem. 266 (2018) 498–507. https://doi.org/10.1016/j.foodchem.2018.06.057.

[19] Y. Zhang, Q. Yu, Y. Liu, et al., Dual cryoprotective and antioxidant effects of young apple polyphenols on myofibrillar protein degradation and gelation properties of bighead carp mince during frozen storage, J. Food Sci. 88 (2023) 4560–4573. https://doi.org/10.1111/1750-3841.16781.

[20] Y. Li, X. Han, Y. Zhang, et al., Thawed drip and its membrane-separated components: role in retarding myofibrillar protein gel deterioration during freezing-thawing cycles, Food Res. Int. 188 (2024) 114461. https://doi.org/10.1016/j.foodres.2024.114461.

[21] Y. Xu, W. Xia, Q. Jiang. Aggregation and structural changes of silver carp actomyosin as affected by mild acidification with *D*-gluconic acid *δ*-lactone, Food Chem. 134 (2012) 1005–1010. https://doi.org/10.1016/j.foodchem.2012.02.21.

[22] K. Xie, F. Yang, X. E. Ren, et al., Insight into the effects of hydrodynamic cavitation at different ionic strengths on

physicochemical and gel properties of myofibrillar protein from tilapia (*Oreochromis niloticus*), Foods 13 (2024) 851. https://doi.org/10.3390/foods13060851.

[23] L. Cai, L. Nian, A. Cao, et al., Effect of carboxymethyl chitosan magnetic nanoparticles plus herring antifreeze protein on conformation and oxidation of myofibrillar protein from red sea bream (*Pagrosomus major*) after freeze-thaw treatment, Food Bioprocess Tech. 13 (2020) 355–366. https://doi.org/10.1007/s11947-019-02384-x.

[24] D. Wu, Y. Cao, T. Yin, et al., Inhibitive effect of trehalose and sodium pyrophosphate on oxidation and structural changes of myofibrillar proteins in silver carp surimi during frozen storage, Food Res. Int. 187 (2024) 114361. https://doi.org/10.1016/j.foodres.2024.114361.

[25] M. Saito, Y. Takenouchi, N. Kunisaki, et al., Complete primary structure of rainbow trout type I collagen consisting of α1(I)α2(I)α3(I) heterotrimers, Eur. J. Biochem. 268 (2001) 2817–2827. https://doi.org/10.1046/j.1432-1327.2001.02160.x.

[26] A. A. Jaziri, R. Shapawi, R. A. M. Mokhtar, et al., Extraction and characterization of type I collagen from parrotfish (*Scarus sordidus* Forsskål, 1775) scale solubilized with the aid of acetic acid and pepsin, Int. J. Biomater. 2023 (2023) 7312447. https://doi.org/10.1155/2023/7312447.

[27] K. Sato, T. Ebihara, E. Adachi, et al., Possible involvement of aminotelopeptide in self-assembly and thermal stability of collagen I as revealed by its removal with proteases, J. Biol. Chem. 275 (2000) 25870–25875. https://doi.org/10.1074/jbc.M003700200.

[28] F. Li, B. Wang, Q. Liu, et al., Changes in myofibrillar protein gel quality of porcine *longissimus* muscle induced by its stuctural modification under different thawing methods, Meat Sci. 147 (2019) 108–115. https://doi.org/10.1016/j.meatsci.2018.09.003.

[29] S. Gao, Y. Liu, Z. Fu, et al., Uncovering quality changes of salted bighead carp fillets during frozen storage: the potential role of time-dependent protein denaturation and oxidation, Food Chem. 414 (2023) 135714. https://doi.org/10.1016/j.foodchem.2023.135714.

[30] L. Cai, L. Nian, G. Zhao, et al., Effect of herring antifreeze protein combined with chitosan magnetic nanoparticles on quality attributes in red sea bream (*Pagrosomus major*), Food Bioprocess Tech. 12 (2019) 409–421. https://doi.org/10.1007/s11947-018-2220-4.

[31] X. Feng, X. Yu, Y. Yang, et al., Improving the freeze-thaw stability of fish myofibrils and myofibrillar protein gels: current methods and future perspectives, Food Hydrocoll. 144 (2023) 109041. https://doi.org/10.1016/j.foodhyd.2023.109041.

[32] Q. Jiang, N. Nakazawa, Y. Hu, et al., Changes in quality properties and tissue histology of lightly salted tuna meat subjected to multiple freeze-thaw cycles, Food Chem. 293 (2019) 178–186. https://doi.org/10.1016/j.foodchem.2019.04.091.

[33] H. H. H. Mohammed, L. He, A. Nawaz, et al., Effect of frozen and refrozen storage of beef and chicken meats on inoculated microorganisms and meat quality, Meat Sci. 175 (2021) 108453. https://doi.org/10.1016/j.meatsci.2021.108453.

[34] X. Du, P. Chang, J. Tian, et al., Effect of ice structuring protein on the quality, thermal stability and oxidation of mirror carp (*Cyprinus carpio* L.) induced by freeze-thaw cycles, LWT-Food Sci. Technol. 124 (2020) 109140. https://doi.org/10.1016/j.lwt.2020.109140.

[35] S. Selli, G. G. Cayhan, Analysis of volatile compounds of wild gilthead sea bream (*Sparus aurata*) by simultaneous distillation-extraction (SDE) and GC-MS, Microchem. J. 93 (2009) 232–235. https://doi.org/10.1016/j.microc.2009.07.010.

[36] X. F. Zhu, N. Zhang, W. F. Lin, et al., Freeze-thaw stability of pickering emulsions stabilized by soy and whey protein particles, Food Hydrocoll. 69 (2017) 173–184. https://doi.org/10.1016/j.foodhyd.2017.02.001.

[37] Z. Song, Y. Yang, F. Chen, et al., Effects of concentration of soybean protein isolate and maltose and oil phase volume fraction on freeze-thaw stability of Pickering emulsion, Foods 11 (2022) 4018. https://www.mdpi.com/2304-8158/11/24/4018.

[38] K. Zhu, Z. Zheng, Z. Dai, Identification of antifreeze peptides in shrimp byproducts autolysate using peptidomics and bioinformatics, Food Chem. 383 (2022) 132568. https://doi.org/10.1016/j.foodchem.2022.132568.

[39] S. Ali, W. Zhang, N. Rajput, et al., Effect of multiple freeze-thaw cycles on the quality of chicken breast meat, Food Chem. 173 (2015) 808–814. https://doi.org/10.1016/j.foodchem.2014.09.095.

[40] C. Xu, Z. Liang, D. Tang, et al., Gas chromatography-mass spectrometry (GC-MS) analysis of volatile components from guava leaves, J. Essent. Oil Bear. Pl. 20 (2017) 1536–1546. https://doi.org/10.1080/0972060X.2017.1417746.

[41] H. Li, Y. Wang, J. Zhang, et al., Prediction of the freshness of horse mackerel (*Trachurus japonicus*) using E-nose, E-tongue, and colorimeter based on biochemical indexes analyzed during frozen storage of whole fish, Food Chem. 402 (2023) 134325. https://doi.org/10.1016/j.foodchem.2022.134325.

[42] M. Iwamura, R. Koyama, Y. Nonaka, et al., High-throughput evaluation system based on fluorescence intensity distribution analysis-polarization to investigate carbohydrate-carbohydrate interactions, Bull. Chem. Soc. Jpn. 89 (2016) 617–625. https://doi.org/10.1246/bcsj.20150369.

[43] W. Wang, S. Ma, Q. Shao, et al., Effects of soy protein isolate and inulin conjugate on gel properties and molecular conformation of Spanish mackerel myofibrillar protein, Foods 13 (2024) 2920. https://doi.org/10.3390/foods13182920.

[44] S. Zhang, R. Liang, Y. Zhao, et al., Immunomodulatory activity improvement of pine nut peptides by a pulsed electric field and their structure-activity relationships, J. Agric. Food Chem. 67 (2019) 3796–3810. https://doi.org/10.1021/acs.jafc.9b00760.

[45] Z. Xu, S. Cao, N. Cui, et al., Cryoprotective activity of different characterized fractions isolated from enzymatic hydrolysates of croceine croaker (*Pseudosciaena crocea*), Foods 13 (2024) 1946. https://doi.org/10.3390/foods13121946.

[46] B. Zhang, C. D. Fang, G. J. Hao, et al., Effect of *κ*-carrageenan oligosaccharides on myofibrillar protein oxidation in peeled shrimp (*Litopenaeus vannamei*) during long-term frozen storage, Food Chem. 245 (2018) 254–261. https://doi.org/10.1016/j.foodchem.2017.10.112.

[47] A. Zhou, S. Benjakul, K. Pan, et al., Cryoprotective effects of trehalose and sodium lactate on tilapia (*Sarotherodon nilotica*) surimi during frozen storage, Food Chem. 96 (2006) 96–103. https://doi.org/10.1016/j.foodchem.2005.02.013.

[48] Y. Liu, Y. Tan, Y. Luo, et al., Evidence of myofibrillar protein oxidation and degradation induced by exudates during the thawing process of bighead carp fillets, Food Chem. 434 (2024) 137396. https://doi.org/10.1016/j.foodchem.2023.137396.

[49] S. Jin, Q. Pang, R. Liu, et al., Dietary curcumin decreased lipid oxidation and enhanced the myofibrillar protein structure of the duck (*Anas platyrhynchos*) breast muscle when subjected to storage, LWT-Food Sci. Technol. 133 (2020) 109986. https://doi.org/10.1016/j.lwt.2020.109986.

[50] F. Li, X. Du, B. Wang, et al., Inhibiting effect of ice structuring protein on the decreased gelling properties of protein from quick-frozen pork patty subjected to frozen storage, Food Chem. 353 (2021) 129104. https://doi.org/10.1016/j.foodchem.2021.129104.

[51] R. Domínguez, M. Pateiro, P. E. S. Munekata, et al., Protein oxidation in muscle foods: a comprehensive review, Antioxidants 11 (2022) 60. https://www.mdpi.com/2076-3921/11/1/60.

[52] G. Colombo, M. Clerici, D. Giustarini, et al., A central role for intermolecular dityrosine cross-linking of fibrinogen in high molecular weight advanced oxidation protein product (AOPP) formation, BBA-Gen. Subjects 1850 (2015) 1–12. https://doi.org/10.1016/j.bbagen.2014.09.024.

[53] F. Yang, W. Jiang, X. Chen, et al., Investigation on the quality regulating mechanism of antifreeze peptides on frozen surimi: from macro to micro, Food Res. Int. 163 (2023) 112299. https://doi.org/10.1016/j.foodres.2022.112299.